Appl Phys B (2011) 105:607–612
DOI 10.1007/s00340-011-4500-9

Applied Physics B
Lasers and Optics

Variable high-energy-laser attenuator based on the interference on a transparent plate

P. Gregorčič · A. Babnik · J. Možina

Received: 23 October 2010 / Revised version: 19 February 2011 / Published online: 7 April 2011

Abstract The transmittance of a transparent plate is theoretically and experimentally investigated, taking into account Fabry–Perot effects due to Fresnel reflections of a Gaussian beam on the boundaries of a plate. On the basis of these theoretical and experimental predictions, we present the application of a variable laser attenuator based on a thin transparent plate and a temperature regulation. Here, the absorption of the laser energy in the plate should be as low as possible, and its transmittance is changed by the interference due to the different thicknesses and refractive indices for the different temperatures of the plate. Therefore, such an attenuator can be used for a broad range of wavelengths and high-energy laser applications.

1 Introduction

The ideal laser attenuator should enable a uniform power reduction over a wide dynamic range, should not significantly affect the beam's polarization and geometrical (diameter, divergence, intensity profile, direction) properties [1], and should have a simple, robust, and inexpensive mechanical and optical design [2]. In the case of a high-energy-laser attenuator, the main obstacles arise from damage and heating instabilities [3]. Since these phenomena are strongly related with the absorption of laser energy, the absorption of the laser light within the attenuator should be as low as possible, especially in high-power laser systems.

This paper describes the attenuation of laser beam by a transparent plate. Here, the attenuation is achieved by the interference of the multiple reflected beams due to Fresnel reflections on the plate's surfaces rather than by the absorption within the plate. Since no coating is involved, such an attenuator enables high-power handling and can be used for a broad range of wavelengths. However, an appropriate plate material should be selected (e.g., borosilicate glass for visible light and near IR, or sapphire for near and middle UV) in order to avoid the absorption within the plate. The variation of attenuation can be achieved by changing the number of plates being utilized, by a tilt of a single window [4, 5], or by changing the thickness of a single window [6]. Our experiments show that changing the thickness of the plate by heating is the most promising technique to achieve the precise variation of laser-light attenuation with interference on a transparent plate. Additionally, with this technique a very accurate and consequently complex and expensive tilting mechanism [1] can be avoided.

The widest dynamic range of the attenuation by the interference effects at a transparent plate is achieved at large incident angles of the laser beam. Unfortunately, large incident angles cause noticeable beam's parallel shift and also spoil the beam's intensity profile when a thick plate is used. To avoid this unwanted effects, we used a thin (140 µm) transparent plate in our experiments. We also present how small wedge angles of the transparent plate reduce the dynamic range of the interference attenuator. Although this effect is often neglected [4], it is not negligible.

2 Attenuation principle

A transparent plate made using a material with the refractive index n and thickness d can be considered as a Fabry–Perot etalon having two reflecting surfaces that have the reflectivity $R(\theta_i)$ and are separated by a distance d (see Fig. 1). The

P. Gregorčič (✉) · A. Babnik · J. Možina
Faculty of Mechanical Engineering, University of Ljubljana,
Aškerčeva 6, 1000 Ljubljana, Slovenia
e-mail: peter.gregorcic@fs.uni-lj.si

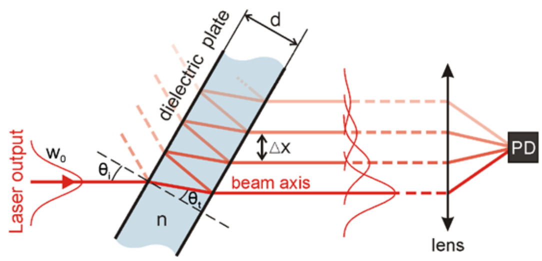

Fig. 1 The propagation of a Gaussian beam through the dielectric plate of thickness d and refractive index n. Lines represent the axes of successively transmitted beams. During the measurement, all the intensity of the transmitted beams is collected on a photo-detector (PD)

surface reflectivity $R(\theta_i)$ depends on the incident angle θ_i and polarization of the light, and can be described by Fresnel equations:

$$\begin{aligned} R(\theta_i) &= \frac{I_s}{I} R_s(\theta_i) + \frac{I_p}{I} R_p(\theta_i), \\ R_s &= \left(\frac{\sin(\theta_t - \theta_i)}{\sin(\theta_t + \theta_i)}\right)^2, \qquad R_p = \left(\frac{\tan(\theta_t - \theta_i)}{\tan(\theta_t + \theta_i)}\right)^2. \end{aligned} \tag{1}$$

Here, the subscripts s and p stand for the linear polarizations perpendicular (s-polarization) and parallel (p-polarization) to the plane of incidence, respectively; I is the incident intensity; and the angle of refraction θ_t can be calculated using Snell's law. The intensities for both polarizations are denoted by I_s and I_p, respectively.

When a monochromatic laser light is incident upon a transparent plate, multiple reflections take place inside the plate, leading to successive reflected and transmitted beams. If the laser beam can be described as the fundamental mode of a coherent Gaussian beam and the absorption within the plate is neglected, the power transmittance of the interference attenuator can be calculated using the Jones matrices [6]. Since a detailed theoretical derivation can be found in [6], we will show here only the final results.

Figure 1 shows a Gaussian beam that is incident upon a dielectric plate, making an angle θ_i with the surface normal. From the geometry presented in Fig. 1, it can be seen that the transverse displacement

$$\Delta x = 2d \tan\theta_t \cos\theta_i \tag{2}$$

between the two adjacent, reflected beams appears in addition to the path difference δ between the successive transmitted beams:

$$\delta = 2kdn \cos\theta_t. \tag{3}$$

Here, $k = 2\pi/\lambda$ is the wave number, and λ stands for the wavelength of the laser light in the vacuum.

The power-transmission coefficient for a Gaussian beam with the beam-waist radius w_0 propagating through the transparent plate can be described by [6]:

$$\begin{aligned} T_P^{(G)} &= (1 - R(\theta_i))^2 \sum_{l=0}^{\infty} \sum_{m=0}^{\infty} R(\theta_i)^{m+l} \\ &\quad \times \exp\left\{-\frac{\Delta x^2}{2w_0^2}(m-l)^2\right\} \cos((m-l)\delta). \end{aligned} \tag{4}$$

In the limit of the plane wave ($w_0 \to \infty$), the term in the curly brackets in (4) goes to zero, and the power-transmission coefficient for the dielectric plate yields the well-known Airy function [7]:

$$T_P^{(PW)} = \frac{1}{1 + \frac{4R(\theta_i)}{(1-R(\theta_i))^2} \sin^2(\delta/2)}, \tag{5}$$

where $T_P^{(PW)}$ stands for the power-transmission coefficient for a plane wave.

On the other hand, if the light is incoherent, there is no interference between successively transmitted beams and the transmittance of a transparent plate can be described as:

$$T_P^{(NC)} = (1 - R)^2 \sum_{l=0}^{\infty} R^{2l} = \frac{(1 - R(\theta_i))^2}{1 - R(\theta_i)^2}. \tag{6}$$

Figure 2 shows theoretical transmittance of a coherent light as a function of the incident angle. Calculations were performed for the laser wavelength $\lambda = 633$ and refractive index $n = 1.52$. Theoretical results were determined for both polarizations, different beam-waist radii and different thicknesses of the plate in order to show the influence of the polarization of incident light, the influence of the plate thickness on the period of oscillations, and the influence of the ratio between the plate thickness d and the beam waist radius w_0. The black line in Fig. 2 shows theoretical result for an incoherent light, defined by (6).

The comparison between the s- (Fig. 2(a)–(c)) and p-polarization (Fig. 2(d)–(f)) of the incident light reveals that the polarization plays an important role due to the existence of Brewster angle θ_B, defined as $\tan(\theta_B) = n$. In the case of the p-polarized light, the incident light is perfectly transmitted through the plate, with no reflections, when the incident angle is equal to the Brewster angle. Therefore, at that angle the transmittance oscillations disappear.

Equation (3) shows that the phase-shift difference between the successive transmitted beams with respect to the incident angle depends on the thickness d of the plate. Figure 2 shows theoretical results for plates with thicknesses of 0.14, 0.42, and 0.7 mm. From these results one can see that the period of oscillations increases with the plate's thickness.

The term in the curly bracket in (4) shows that the interference oscillations depend on the ratio between the plate's thickness d and the beam waist radius w_0. If this ratio is

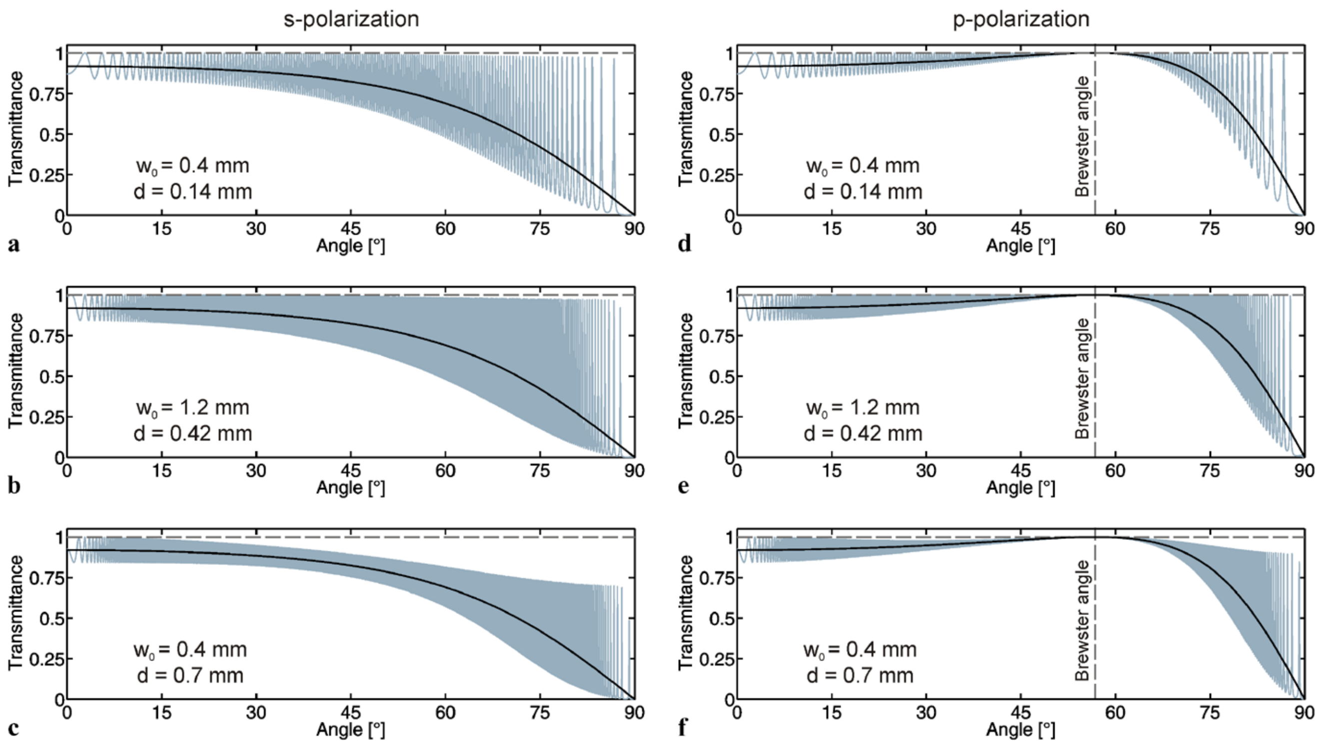

Fig. 2 Theoretical transmittance as a function of the incident angle for s- and p-polarization. The transmittance is shown for different thicknesses of the plate d as well as for two different beam-waist radii w_0. The *solid black curve* shows the transmittance for incoherent light (see (6))

much smaller than 1, the results are similar to results for the plane wave, which is not spatially limited, and therefore the peak values of transmittance oscillations are near 1 for all the incident angles. This phenomenon can be seen from results, shown in Fig. 2(a), (b), (d), and (e), which are calculated for the ratio $d/w_0 = 0.35$. On the other hand, increasing the ratio d/w_0 decreases the peak values of interference oscillations at large angles, as can be seen from Fig. 2(c) and 2(f). This happens because the Gaussian beam is spatially limited, and therefore the successively reflected and transmitted beams are only partially overlapped.

The overlapping between the reflected beams depends on the transverse displacement Δx, defined by (2). This transverse displacement for a 5-mm-thick dielectric plate as a function of the incident angle is shown in Fig. 3(a). It has a maximum for the incident angle

$$\theta_i = \arcsin\sqrt{n^2 - n\sqrt{n^2-1}}$$

($\theta_i = 49°$ for $n = 1.52$), and at that angle the maximum transverse displacement equals

$$\Delta x_{\max} = 2d\sqrt{2n^2 - 1 - 2n\sqrt{n^2-1}}$$

($\Delta x_{\max} = 3.75$ mm for 5-mm-thick plate).

Figure 3(b) shows theoretical transmittance of a 5-mm-thick transparent plate as a function of incident angle. In this case, the interference oscillations for the beam with the radius of 0.4 mm occur only for incident angles $\theta_i < 13°$ and $\theta_i > 81°$. At all other angles the transverse displacement Δx is larger than the beam diameter ($2w_0$), and therefore successively transmitted beams do not overlap anymore and, consequently, the interference oscillations disappear.

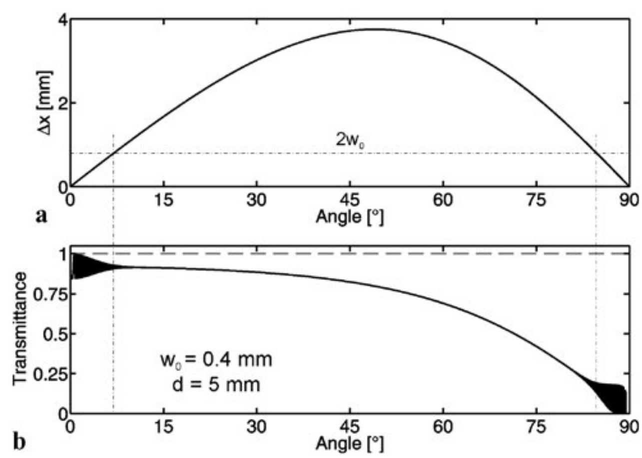

Fig. 3 (**a**) Evolution of the transverse displacement Δx as a function of incident angle for the 5-mm-thick plate with $n = 1.52$. (**b**) Theoretical transmittance as a function of incident angle for the beam with radius 0.4 mm and the 5-mm-thick plate with $n = 1.52$

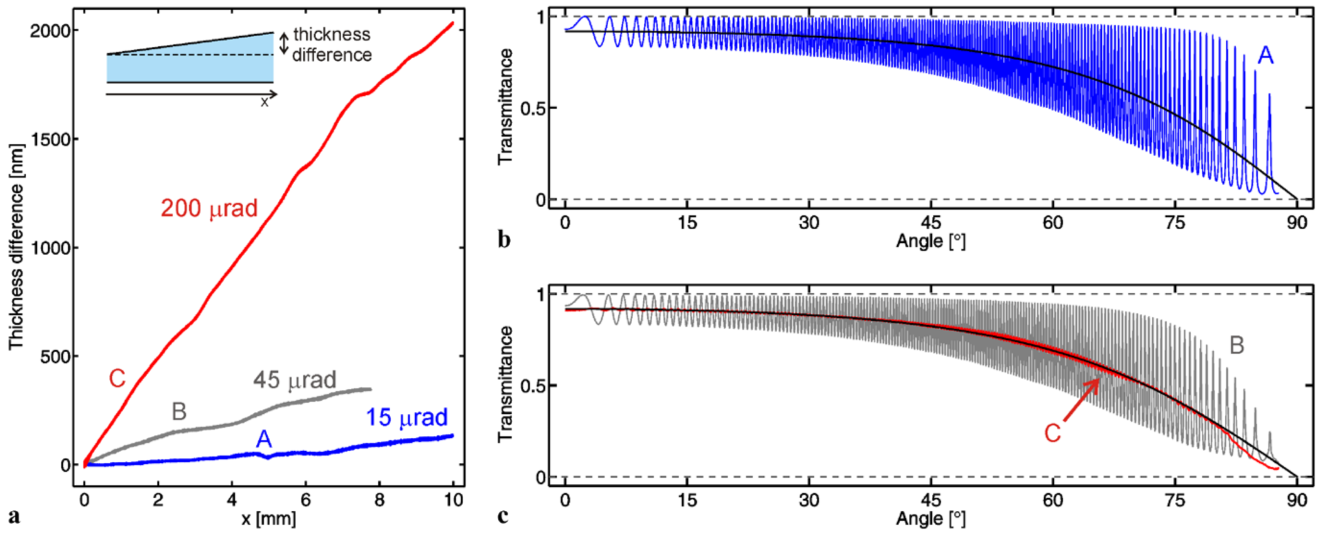

Fig. 4 (**a**) The measured parallelism for all tested plates. (**b**) The measured transmittance as a function of incident angle for the plate with parallelism of 15 µrad. (**c**) The measured transmittance for the plates with parallelism of 45 µrad (the *gray curve*) and 200 µrad (the *red curve*). The *black curves* show the theoretical result for incoherent light (see (6))

3 Measured transmittance as a function of incident angle

For the measurements of the interference phenomena due to Fresnel reflections on the boundaries of a dielectric plate, we used a 140-µm-thick polished borosilicate glass plate with a refractive index $n = 1.52$. The flatness of the plate was $\lambda/10$ at 633 nm. We tested three plates with equal thickness and flatness, but different parallelism. The parallelism was measured by a homodyne quadrature laser interferometer [8]. Here we measured the thickness difference along the plate (see the inset in Fig. 4(a)). Results for all three plates are shown in Fig. 4(a)—the measured parallelism was 200, 45, and 15 µrad for the individual plates.

Transmission measurements as a function of the incident angle were performed with the He–Ne laser beam ($\lambda = 633$ nm) using the beam-waist radius $w_0 = 400$ µm. The spot size on the plate was $w = 448$ µm, and the radius of curvature was $\rho = 1.98$ m. The cylindrical head of the polarized He–Ne laser was rotated so that the linear polarization of the probe beam was perpendicular to the plane of incidence (s-polarization). The plate, maintained at a constant room temperature, was rotated around the vertical axes with a constant angular velocity. The transmitted light was collected by a lens and measured by a photodiode located at the focus of the lens. In this way, the transmission of the plate was measured as a function of the incident angle θ_i. Experimental results for all tested plates are shown in Fig. 4(b) and (c).

Figure 4(b) shows the measured transmittance for the plate with a parallelism of 15 µrad. A comparison of these results with the corresponding theoretical results in Fig. 2(a) reveals a good agreement between the experiment and the theory. However, in contrast to the theoretical predictions, the experimental results show a larger decrease in the interference maxima at large angles. This happens because the dielectric plate's surfaces are not perfectly parallel; instead, they form a small wedge. The wedge changes the plate's thickness, so particular points of the probe-beam profile experience different transmittance. This has been proven by measuring the transmittance of plates with equal thickness and flatness, but different parallelisms.

The gray and the red curves in Fig. 4(c) show the measured transmittance for the plates with parallelisms of 45 and 200 µrad, respectively. It is clear that the interference maxima decrease when the wedge increases from 15 µrad (the gray curve in Fig. 4(b)) to 45 µrad (the gray curve in Fig. 4(c)). In the case of the plate with a parallelism of 200 µrad, i.e., the 200-nm change in plate's thickness at 1 mm, which approximately corresponds to a $\lambda/4$-change of the plate's thickness within the probe-beam diameter, the measured transmittance conforms to the transmittance of the incoherent light. This phenomenon can be seen by a comparison between the black and the red curves in Fig. 4(c). Here, the solid black curve shows theoretical transmittance for the incoherent light (see (6)). From measured results in Fig. 4 it can be concluded that small wedges reduce the interference fringes, and therefore reduce the dynamic range of a transparent plate applied as an interference attenuator.

When a transparent plate is applied as an interference attenuator, the attenuation can be changed by the incident angle, as was shown with the theoretical results in Fig. 2 as well as with the experimental results presented in Fig. 4. Therefore, we measured the transmittance of a pulsed Nd:YAG laser (Quantel, Brio, $\lambda = 1064$ nm) as a function

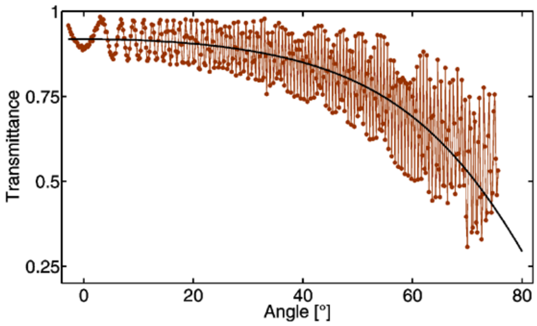

Fig. 5 The measured transmittance of a pulsed Nd:YAG laser as a function of incident angle. Each point is an average of 50 measurements. The black curve shows the theoretical result for incoherent light (see (6))

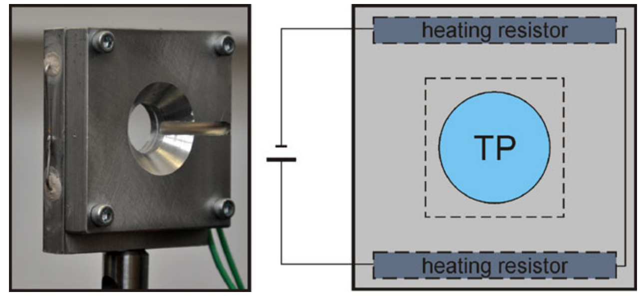

Fig. 6 A prototype of an attenuator based on the temperature-dependent interference effects. The 140-μm-thick transparent plate (TP) is put between two 8-mm-thick aluminum layers. Heating-resistors are used for temperature regulation

of the incident angle. The laser pulses with duration of 4 ns had energy of 100 mJ. Measurements, performed in steps of 0.2°, are shown in Fig. 5. Each point is an average of 50 measurements. From these experimental results it can be estimated that the full-width-at-half-maximum for a single fringe is about 0.5°. Therefore, it can be concluded that this technique requires a precise positioning system.

4 Application of a laser attenuator

Measured and theoretical results, presented in previous sections, show that it is difficult to control the plate's transmittance with the incident angle. A more accurate manipulation can be achieved by changing the plate's thickness. This can be done most conveniently by heating the dielectric plate.

The change of a phase-shift difference for one round trip in the plate, δ, in a linear approximation depends on the plate's temperature change as:

$$\delta(\Delta T) \approx 2kn_0d_0\left(1+\left(\alpha+\frac{\partial n}{\partial T}\right)\Delta T\right)\cos(\theta_t). \qquad (7)$$

Here, ΔT denotes the temperature change; n_0 and d_0 are initial refractive index and the plate's thickness, respectively; α is the linear temperature coefficient; and $\partial n/\partial T$ shows the change of the refractive index with the plate's temperature.

Figure 6 shows a prototype of the attenuator based on the temperature-dependent interference effects at a transparent plate. Here the 140-μm-thick borosilicate glass plate is put between two 8-mm-thick aluminum layers. The plate is heated by heating-resistors which are inside the aluminum layers and can heat the plate from the room temperature to 120°C. The reason that we have chosen a 140-μm-thick plate is that a thin plate does not significantly distort the intensity profile of the transmitted beam. Another reason is that the parallel shift of the incident beam depends on the plate's thickness as $\Delta X = d\cos(\theta_i)(\tan(\theta_i) - \tan(\theta_t))$. Therefore,

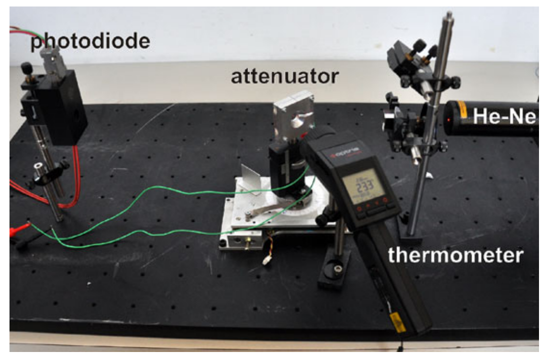

Fig. 7 Experimental setup for measurements of the attenuator's transmittance

in the case of 140-μm-thick borosilicate plate, this displacement of an attenuated laser beam is small ($\Delta X < 100$ μm for incident angles $\theta_i < 70°$). Furthermore, since the incident angle is constant during the variation of the attenuation, the parallel shift of the incident laser beam is also constant for the whole range of the attenuation.

The transmittance of the described interference attenuator as a function of the temperature was measured by the experimental setup, shown in Fig. 7. We measured the transmittance at different plate's temperatures obtained by different powers of the heating-resistors. The plate's temperature during the experiment was measured by the infrared thermometer (Optris, LaserSight).

The measured attenuator's transmittance as a function of the temperature for the incident angle $\theta_i = 68°$ is shown in Fig. 8. The transmittance changes periodically with the period of ~150 K, while the measured transmittance is in the interval between 0.35 and 0.96. The black curve shows a theoretical fit according to (5), where the temperature-dependent phase-shift difference $\delta(\Delta T)$, defined by (7), is involved. The difference in the peak values between the fitted (the black curve) and the measured transmittance appears because the limited-beam and the wedge effects are not taken into account in (5).

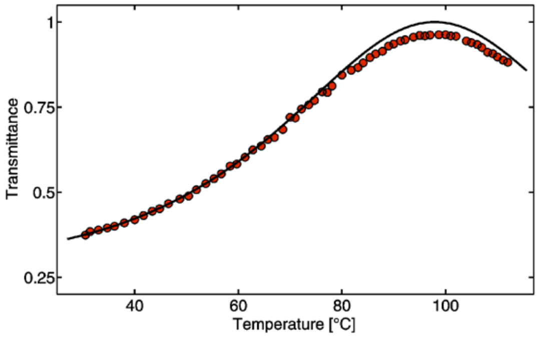

Fig. 8 Measured transmittance as a function of the temperature for the incident angle $\theta_i = 68°$. The *black curve* shows the theoretical fit

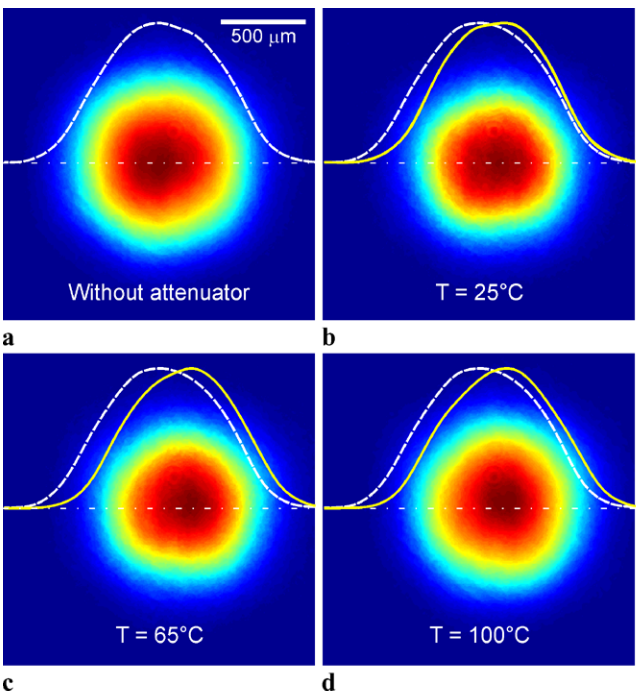

Fig. 9 Measured intensity profiles of the transmitted beam (**a**) without an attenuator, and (**b**)–(**d**) with the attenuator at different temperatures

We have chosen the incident angle of 68° because at this angle the applied plate has the widest dynamic range. As was shown in previous sections, the dynamic range increases with the incident angle (see Figs. 2(a) and 4(b)). However, in order to achieve a wide dynamic range, a plate, which thickness changes less than 20 nm within the beam's diameter (i.e., less than 20 µrad for the beam diameter of 1 mm), should be used, as has been shown with experimental results in Fig. 4.

We also measured the intensity profile of the transmitted He–Ne laser-beam during our experiments. For this case, the photodiode in Fig. 7 was replaced with a CCD camera. The profile, measured without an attenuator, is shown in Fig. 9(a), where the 1D-profile across the dot-dashed line is shown with the white dashed curve. The dot-dashed line is parallel to the optical table (see Fig. 7), and the scale is shown with the white bar. Then the attenuator, maintained at room temperature, was placed into the measuring setup. Figure 9(b) shows the intensity profile for this case. Here, it can be seen that the parallel shift of the incident laser beam is approximately $\Delta X \sim 90$ µm, which corresponds to the theoretical results for the 140-µm-thick borosilicate plate and $\theta_i = 68°$. Figures 9(c) and (d) show the intensity profile of the transmitted beam during the heating of the plate. The white dashed curves in Fig. 9(b)–(d) correspond to the 1D-intensity profile of the used He–Ne laser without the attenuator (the 1D-profile from Fig. 9(a)), while the solid yellow curves show the 1D-profile (across the dot-dashed line) of the beam transmitted through the attenuator. The intensity profiles in Fig. 9 are normalized. In the direction perpendicular to the optical table, the intensity profile does not change significantly during the measurements.

5 Conclusions

The interference effects of a tilted transparent plate for an incident Gaussian beam have been theoretically and experimentally investigated, taking into account the Fabry–Perot effects due to Fresnel reflections on the plate's boundaries. The presented results show a typical behavior of multiple-reflected beams interfering with each other, which manifests itself in the plate's transmittance oscillations.

We have shown that these transmittance oscillations depend on the incident angle, and therefore can be used for an attenuation of continuous-wave- and pulsed-laser light. However, our results reveal that in this case a precise positioning system is required. Therefore, we proposed a more accurate manipulation of plate's transmittance by the heating of the plate. Here we have shown a prototype of a variable laser attenuator based on the temperature-dependent interference effects, which can be used for high-power laser applications. Moreover, we have shown that in this case small wedge angles of the plate play an important role, since they reduce the dynamic range of such an attenuator.

References

1. K. Bennett, R.L. Byer, Appl. Opt. **19**, 2408 (1980)
2. J. Staromlynska, R.A. Clay, K.F. Dexter, Appl. Opt. **26**, 3827 (1987)
3. R.O. Rice, J.D. Macomber, Appl. Opt. **14**, 2203 (1975)
4. J.C. Cotteverte, F. Bretenaker, A. Le Floch, Appl. Opt. **30**, 305 (1991)
5. R.M.A. Azzam, Appl. Opt. **48**, 425 (2009)
6. P. Gregorčič, A. Babnik, J. Možina, Opt. Express **18**, 3871 (2010)
7. H. Abu-Safia, R. Al-Tahtamouni, I. Abu-Aljarayesh, N.A. Yusuf, Appl. Opt. **33**, 3805 (1994)
8. P. Gregorčič, T. Požar, J. Možina, Opt. Express **17**, 16322 (2009)